Solid-State Electronics 54 (2010) 605–608

Contents lists available at ScienceDirect

Solid-State Electronics

journal homepage: www.elsevier.com/locate/sse

High efficient organic ultraviolet photovoltaic devices based on gallium complex

Zisheng Su [a,b], Bei Chu [a], Wenlian Li [a,*]

[a] Key Laboratory of Excited State Processes, Changchun Institute of Optics, Fine Mechanics and Physics, Chinese Academy of Sciences, Changchun 130033, People's Republic of China
[b] Graduate School of Chinese Academy of Sciences, Beijing 100039, People's Republic of China

ARTICLE INFO

Article history:
Received 25 September 2009
Received in revised form 28 January 2010
Accepted 28 January 2010
Available online 21 February 2010

The review of this paper was arranged by editor Prof. A. Zaslavsky

Keywords:
Organic photovoltaic devices
Geminate electron–hole pair
Exciplex

ABSTRACT

High efficient organic ultraviolet (UV) photovoltaic devices comprising 4,4′,4″-tri-(2-methylphenyl phenylamino) triphenylamine (m-MTDATA) and tris-(8-hydroxyquinoline) gallium (Gaq_3) as the electron donor and acceptor, respectively, are demonstrated. The m-MTDATA/Gaq_3 bilayer device shows a short-circuit current density of 59.3 $\mu A/cm^2$, a open-circuit voltage of 1.85 V, a fill factor of 0.41, and a power conversion efficiency of 3.74% under illumination of a 1.2 mW/cm^2 365 nm UV light. And this power conversion efficiency is superior than that of the device based on tris-(8-hydroxyquinoline) aluminum with the same device structure, which is attributed to the high electron mobility of Gaq_3 and the low exciton loss via radiation decay and hence more exciton dissociation in m-MTDATA/Gaq_3 device.

1. Introduction

In the past two decades, there is a growing interest on organic electronic devices, including light-emitting diodes [1], photovoltaic (PV) devices [2], thin film transistors [3], etc., due to their light weight, low cost, and compatibility with flexible substrates compared to inorganic counterparts. Since the demonstration of high efficient exciton dissociation in the donor–acceptor (D–A) heterojunction interface [4], PV devices have drawn particular attention owing to their potential applications in solar cells and photodetectors [5–9]. The PV effect involves the formation of excitons under illumination, the diffusion of excitons to the D–A interface, the dissociation of excitons into electrons and holes, and the collection of electrons and holes at opposite electrodes. To achieve a maximum efficiency, many methods have been adopted to optimize all the four processes involved in the generation of photocarriers [10–12].

The major ultraviolet (UV) radiation reaching the surface of the earth covers wavelength from 300 to 420 nm, and a lot of diseases, such as skin cancer, would be caused by long-term exposure to the UV radiation. Thereby it is necessary to detect the UV radiation intensity for human health. On the other hand, UV PV devices have the potential applications for UV curing monitors, solar astronomy, missile plume detection, and space-to-space transmission. Thus, they are attracting much attention recently. UV PV devices comprising a lot of materials have been reported, such as rear-earth complexes [13–15], Cu(I) complexes [16], and polymer/inorganic hybrids [17]. Hong et al. [18] reported that PV devices with 4,4′,4″-tri-(2-methylphenyl phenylamino) triphenylamine (m-MTDATA) and tris-(8-hydroxyquinoline) aluminum (Alq_3) acted as the electron donor and acceptor, respectively. Tris-(8-hydroxyquinoline) gallium (Gaq_3) has analogous molecular structure and photophysical properties to that of Alq_3. The photoluminescent (PL) quantum efficiency of Gaq_3 is demonstrated to be a quarter of that of Alq_3 [19,20]. Low PL efficiency of the donor and the acceptor is usually considered as one criterion to obtain high power conversion efficiency (η_P) in PV devices due to the competitive processes of the exciton radiation and exciton dissociation. Moreover, the electron mobility of Gaq_3 is higher than that of Alq_3 [19,21]. In view of these, Gaq_3 may offer superior performance compared to Alq_3 in the PV devices. In this paper, UV PV devices with m-MTDATA as the electron donor and Gaq_3 as the electron acceptor, respectively, were fabricated. The m-MTDATA/Gaq_3 bilayer device shows a short-circuit current (J_{SC}) of 59.3 $\mu A/cm^2$ and a η_P of 3.74%. And the performance is better than that of Alq_3 with the same device structure, which is attributed to the high electron mobility of Gaq_3 and low exciton loss due to radiation and hence more exciton dissociation in the m-MTDATA/Gaq_3 interface.

2. Experimental

Devices were fabricated on precleaned indium tin oxide (ITO)-coated glass substrates with a sheet resistance of 25 Ω/sq. A 50 nm 3,4-polyethylenedioxythiophene:polystyrenesulfonate (PEDOT:PSS) was spin-coated on ITO, followed by drying at 120 °C for

* Corresponding author. Tel./fax: +86 431 86176345.
E-mail address: wllioel@yahoo.com.cn (W. Li).

0038-1101/$ - see front matter
doi:10.1016/j.sse.2010.01.025

60 min in vacuum. The PEDOT:PSS layer serves to planarize the ITO, thereby preventing shorts through the thin donor and acceptor layers [22]. Then, m-MTDATA and Gaq_3, which acted as the electron donor and acceptor, respectively, were thermal evaporated in vacuum chamber at 3×10^{-4} Pa, followed by a 0.5 nm LiF and 100 nm Al cathode. The molecular structures of m-MTDATA and Gaq_3 are shown in Fig. 1. Two devices were fabricated with configurations as follows:

Device A: ITO/PEDOT:PSS/m-MTDATA (30 nm)/Gaq_3 (30 nm)/LiF /Al
Device B: ITO/PEDOT:PSS/m-MTDATA (30 nm)/Alq_3 (30 nm)/LiF/Al

Deposition rates and thickness of the layers were monitored using oscillating quartz monitors. The evaporating rates were kept at 0.5–1 Å/s for organic layers and LiF layer and 10 Å/s for Al cathode, respectively. Absorption spectra of all organic films on quartz substrates were measured with a Shimadzu UV-3101 PC spectrophotometer. PL spectra were measured with a Hitachi F-4500 spectrophotometer. Photocurrent response curve was obtained under irradiance of a 40 μW/cm^2 Xe lamp. Current density–voltage (*I*–*V*) curves were measured by a Keithley 2400 source meter under illumination of 365 nm UV light (1.2 mW/cm^2) or AM 1.5 solar simulator (100 mW/cm^2). All the measurements were carried out at room temperature under ambient conditions.

3. Results and discussion

Fig. 2 shows the absorption spectra of 30 nm m-MTDATA, 30 nm Gaq_3, 30 nm Alq_3, and 30 nm m-MTDATA/30 nm Gaq_3 blend films on quartz substrates. A broad absorption band in the range of 300 to 400 nm in the absorption spectrum was found in the m-MTDATA/Gaq_3 bilayer film, which is a simple superposition of the absorptions of m-MTDATA and Gaq_3, indicating that the absorptions of m-MTDATA and Gaq_3 are responsible for the photo-induced carrier generation. For reference, the absorption spectrum of 30 nm Alq_3 measured with the same conditions is also presented in Fig. 2. Gaq_3 and Alq_3 have almost the same absorption spectra in the range investigated, although the absorption coefficiency of Alq_3 is a little lower than that of Gaq_3. The photocurrent response curve of Device A is shown in Fig. 3, which reveals a maximum response in the region of 360–370 nm. Thus, a 365 nm UV light was selected as the illumination source for the PV devices.

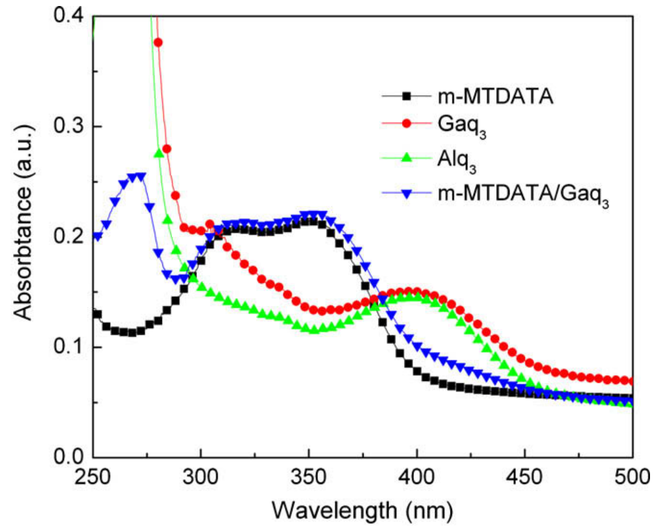

Fig. 2. Absorption spectra of 30 nm m-MTDATA, 30 nm Gaq_3, 30 nm Alq_3, and 30 nm m-MTDATA/30 nm Gaq_3 films on quartz substrates.

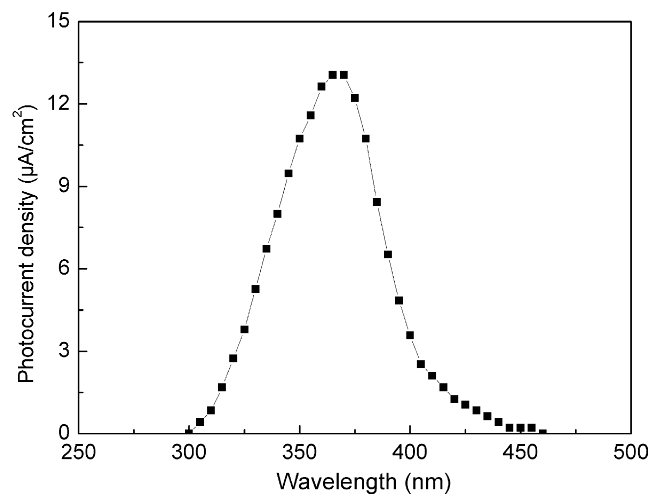

Fig. 3. Photocurrent response of Device A under illumination of a Xe lamp.

Fig. 4 plots the *I*–*V* characteristics of Devices A and B under irradiation of a 365 nm UV light with the intensity of 1.2 mW/cm^2.

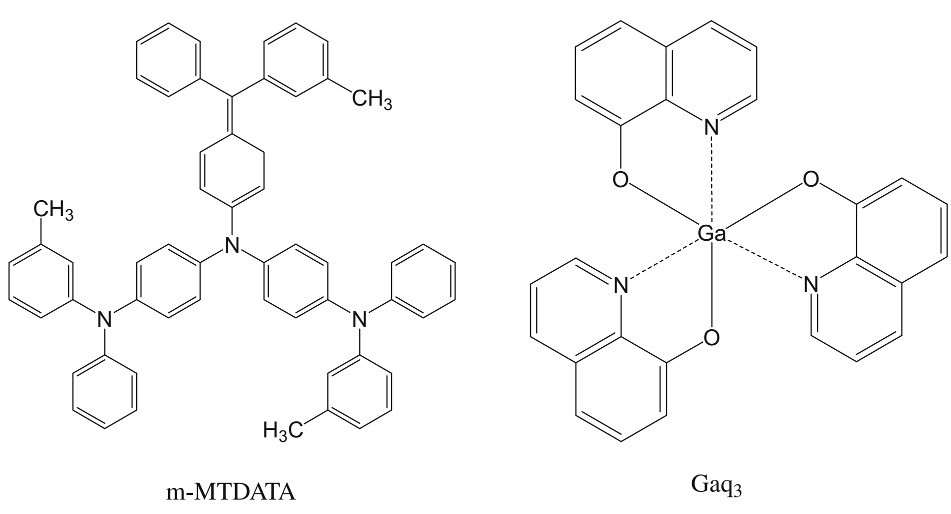

Fig. 1. Molecular structure of m-MTDATA and Gaq_3.

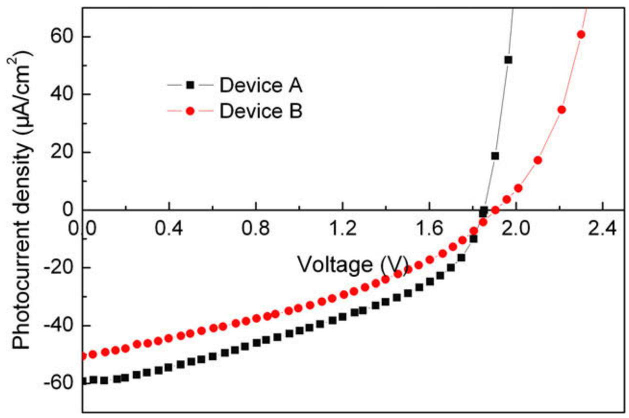

Fig. 4. *I–V* characteristics of Devices A and B under illumination of a 1.2 mW/cm^2 UV light.

Among the two devices, Device A presents the superior performance, which shows a J_{SC} of 59.3 μA/cm^2 and an open-circuit voltage (V_{OC}) of 1.85 V. Calculating the fill factor (*FF*) and η_P from the *I–V* curve with equations

$$FF = \frac{(J \times V)_{max}}{V_{oc} \times J_{SC}} \quad (1)$$

$$\eta_p = \frac{(J \times V)_{max}}{P_{in}} = \frac{FF \times V_{oc} \times J_{SC}}{P_{in}} \quad (2)$$

where $(J \times V)$max is the actual maximum power and P_{in} is the incident light intensity, a *FF* and η_P of 0.41 and 3.74% are achieved, respectively. The J_{SC}, V_{OC}, *FF*, and η_P of Device B are 50.6 μA/cm^2, 1.91 V, 0.37, and 2.94%, respectively. The performance is much higher than the report by Hong et al. [18], which may be attributed to the improved contact between the electrodes and the organic layers and hence the extraction efficiency of hole and electron from the bulk of the organic films due to the incorporations of the PEDOT:PSS and LiF layers [22,23]. The J_{SC}, V_{OC}, *FF*, and η_P of Device A under 100 mW/cm^2 AM 1.5 solar simulation are 353.1 μA/cm^2, 1.87 V, 0.28, and 0.18%, while they are 295.5 μA/cm^2, 1.94 V, 0.27, and 0.16% for Device B, respectively, as shown in Fig. 5. It can be noted that the V_{OC} of the devices is increased and the *FF* is reduced compared to that illuminated by UV light, which are commonly observed in PV devices with increasing irradiation power [22]. The low η_P of Devices A and B is primarily due to they only absorb UV light (as shown in Fig. 2), which accounts for a small fraction of the solar irradiation. Gaq_3 and Alq_3 have almost the same ionization potential and electron affinity [24,25], thus the difference in energy levels can be ruled out for the better performance of Device A. Meanwhile, a little higher absorption of Gaq_3 as presented in Fig. 2 cannot account for such a distinct distinguished performance between these two devices.

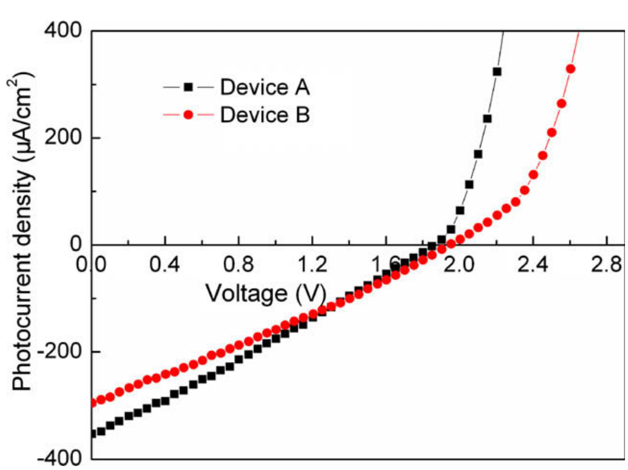

Fig. 5. *I–V* characteristics of Devices A and B under 100 mW/cm^2 AM 1.5 illumination.

PL quenching of the donor and acceptor is always regarded as an indicator of the performance of PV devices. Fig. 6 depicts the PL spectra of 30 nm Alq_3, 30 nm Gaq_3, 60 nm m-MTDATA:Alq_3 (1:1), and 60 nm m-MTDATA:Gaq_3 (1:1) films on quartz substrates with an excitation wavelength of 365 nm. The PL spectra of Alq_3 and Gaq_3 show emission peaks at 512 and 522 nm, respectively. While broadened and red-shifted PL spectra with peaks at about 535 and 537 nm are found in the m-MTDATA:Alq_3 and m-MTDATA:Gaq_3 blend films, respectively, and the PL intensity of the latter is lower than that of the former. The broadened and red-shifted emission of the m-MTDATA:Alq_3 blend film was previously attributed to the hybrid emissions of Alq_3 and the m-MTDATA/Alq_3 interfacial exciplex [18,25]. Thus, emission of the m-MTDATA:Gaq_3 can be similarly ascribed to the hybrid emissions of Gaq_3 and the m-MTDATA/Gaq_3 interfacial exciplex as Gaq_3 has the analogous molecular structure and photophysical properties to that of Alq_3. No emission of m-MTDATA is found in blend films, indicating that nearly all the m-MTDATA excitons have transferred their electron to the donors Alq_3 and Gaq_3.

Recently, a two-step model for charge dissociation, proceeding via the formation of interfacial geminate electron–hole pair (or named as interfacial bound radical pair) is proposed [26–28]. According to this model, electron transfer from the donor to the acceptor forms the geminate electron–hole pairs, and the dissociation of the geminate electron–hole pairs generates free charge carriers, while the recombination of the geminate electron–hole pairs results in the radiation of the interfacial exciplex. Thereby the formation of such geminate electron–hole pair rather than energy transfer from the high energy species to the lower energy one in the D–A interface is more critical to the performance of the PV devices [29]. To obtain high η_P, efficient charge transfer in the D–A interface and effective suppression of the geminate electron–hole pair recombination to the ground state should be ensured. The absent emission of m-MTDATA in the blend films (as shown in Fig. 6) suggests that efficient electron transfer from m-MTDATA excitons to Gaq_3 and Alq_3 molecules takes place in the m-MTDATA/Gaq_3 and m-MTDATA/Alq_3 interfaces. The remained emissions of Gaq_3

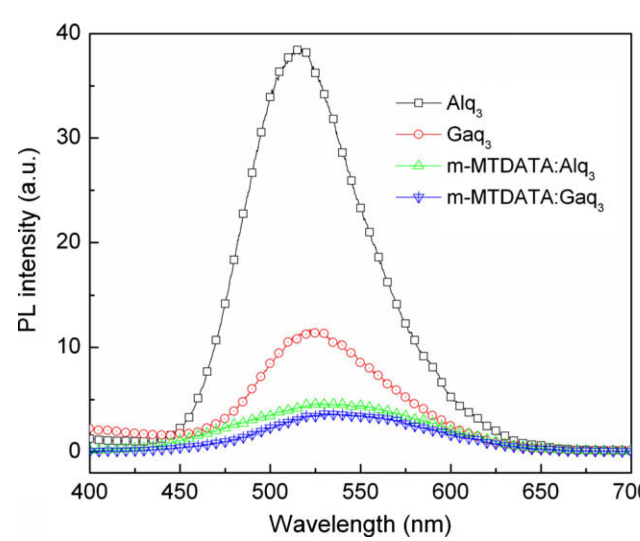

Fig. 6. PL spectra of 30 nm Alq_3, 30 nm Gaq_3, 60 nm m-MTDATA:Alq_3 (1:1), and 60 nm m-MTDATA:Gaq_3 (1:1) films on quartz substrates excited at 365 nm.

or Alq_3 in the blend films indicate that some Gaq_3 or Alq_3 excitons are precluded in the formation of geminate electron–hole pair, and the appearance of exciplexes emission illuminates the recombination of the geminate electron–hole pair. The lower PL emission of the m-MTDATA:Gaq_3 blend film than that of m-MTDATA:Alq_3 indicates low radiation loss in Device A. On the other hand, after the dissociation of the geminate electron–hole pairs, higher electron mobility of Gaq_3 favors the extraction of electron and consequence the dissociation of the geminate electron–hole pairs. Therefore, the combination of low radiation loss and high electron mobility of Gaq_3 is the main cause of the superior performance of Device A than B.

4. Conclusion

In summary, high efficient UV PV devices based on m-MTDATA as the donor and Gaq_3 as the acceptor, respectively, were demonstrated. The m-MTDATA/Gaq_3 bilayer device shows a J_{SC} of 59.3 μA/cm^2, a V_{OC} of 1.85 V, and a η_P of 3.74% under illumination of a 1.2 mW/cm^2 at 365 nm. These findings indicate that Gaq_3 has the potential application in high efficient UV photodetector [30]. Moreover, the performance is better than that of the device based on Alq_3 with the same structure, which is predominantly attributed to the high electron mobility of Gaq_3 and the low radiation loss in Gaq_3 device.

References

[1] Tang CW, VanSkyke SA. Appl Phys Lett 1987;51:913.
[2] Peumans P, Yakimov A, Forrest SR. J Appl Phys 2003;93:3693.
[3] Garnier F, Hajlaoui R, Yassar A, Srivastava P. Science 1994;265:1686.
[4] Tang CW. Appl Phys Lett 1986;48:183.
[5] Yu G, Gao J, Hummelen JC, Wudl F, Heeger AJ. Science 1995;270:1789.
[6] Peumans P, Uchida S, Forrest SR. Nature 2003;425:158.
[7] Li G, Shrotriya V, Huang J, Yao Y, Moriarty T, Emery K, et al. Nat Mater 2005;4:864.
[8] Gunes S, Neugebauer H, Sariciftci NS. Chem Rev 2007;107:1324.
[9] Kim JY, Lee K, Coates NE, Moses D, Nguyen TQ, Dante M, et al. Science 2007;317:223.
[10] Li G, Yao Y, Yang H, Shrotriya V, Yang G, Yang Y. Adv Funct Mater 2007;17:1636.
[11] Bundgaard E, Krebs FC. Sol Enengy Mater Sol Cells 2007;91:954.
[12] Kim JY, Kim SH, Lee HH, Lee K, Ma W, Gong X, et al. Adv Mater 2006;18:572.
[13] Chu B, Fan D, Li WL, Hong ZR, Li RG. Appl Phys Lett 2002;81:10.
[14] Si Z, Li B, Wang L, Yue S, Li W. Sol Enengy Mater Sol Cells 2007;91:1168.
[15] He H, Li W, Su Z, Li T, Su W, Chu B, et al. Solid State Electron 2008;52:31.
[16] Kong Z, Li W, Che G, Chu B, Bi D, Han L, et al. Appl Phys Lett 2006;89:191112.
[17] Li F, Cho SH, Son DI, Kim TW, Lee SK, Cho YH, et al. Appl Phys Lett 2009;94:111906.
[18] Hong ZR, Lee CS, Lee ST, Li WL, Shirota Y. Appl Phys Lett 2002;81:2878.
[19] Burrows PE, Sapochak LS, McCarty DM, Forrest SR, Thompson ME. Appl Phys Lett 1994;64:2718.
[20] Qiao J, Wang LD, Duan L, Li Y, Zhang DQ, Qiu Y. Inorg Chem 2004;43:5096.
[21] Chen BJ, Sun XW, Li YK. Appl Phys Lett 2003;82:3017.
[22] Peumans P, Forrest SR. Appl Phys Lett 2001;79:126.
[23] Hung LS, Tang CW, Mason MG. Appl Phys Lett 1997;70:152.
[24] Wang L, Jiang X, Zhang Z, Xu S. Displays 2000;21:47.
[25] Shirota Y, Kuwabara Y, Inada H, Wakimoto T, Nakada H, Yonemoto Y, et al. Appl Phys Lett 1994;65:807.
[26] Morteani AC, Sreearunothai P, Herz LM, Friend RH, Silva C. Phys Rev Lett 2004;92:247402.
[27] Ohkita H, Cook S, Astuti Y, Duffy W, Tierney S, Zhang W, et al. J Am Chem Soc 2008;130:3030.
[28] Gonzalez-Rabade Astrid, Morteani AC, Friend RH. Adv Mater 2009;21:1.
[29] Veldman D, Meskers SCJ, Janssen RAJ. Adv Funct Mater 2009;19:1929.
[30] Su Z, Li W, Chu B, Li T, Zhu J, Zhang G, et al. Appl Phys Lett 2008;93:103309.